ELSEVIER

Cement & Concrete Composites 22 (2000) 165–174

Cement & Concrete Composites

Improving shear capacity of existing RC T-section beams using CFRP composites

Ahmed Khalifa, Antonio Nanni *

224 Engineering Research Laboratory, Department of Civil Engineering, University of Missouri at Rolla, Rolla, MO 65409, USA

Received 10 May 1999; accepted 8 December 1999

Abstract

This paper presents the shear performance of reinforced concrete (RC) beams with T-section. Different configurations of externally bonded carbon fiber-reinforced polymer (CFRP) sheets were used to strengthen the specimens in shear. The experimental program consisted of six full-scale, simply supported beams. One beam was used as a bench mark and five beams were strengthened using different configurations of CFRP. The parameters investigated in this study included wrapping schemes, CFRP amount, 90°/0° ply combination, and CFRP end anchorage. The experimental results show that externally bonded CFRP can increase the shear capacity of the beam significantly. In addition, the results indicated that the most effective configuration was the U-wrap with end anchorage. Design algorithms in ACI code format as well as Eurocode format are proposed to predict the capacity of referred members. Results showed that the proposed design approach is conservative and acceptable. © 2000 Elsevier Science Ltd. All rights reserved.

Keywords: Bond; Carbon fiber; Composites; Externally bonded reinforcement; Fiber-reinforced polymer (FRP); Reinforced concrete; Repair; Shear strength; Strengthening; T-section

1. Introduction

Recently, innovative composite materials known as fiber-reinforced polymers (FRP) have shown great promise in rehabilitation of existing reinforced concrete (RC) structures. Rehabilitation of these structures can be in the form of strengthening of structural members, repair of damaged structures, or retrofitting for seismic deficiencies. In any case, composite materials are an excellent option to be used as external reinforcing because of their high tensile strength, light weight, resistance to corrosion, high durability, and ease of installation.

Externally bonded FRP reinforcement has been shown to be applicable for the strengthening of many types of RC structures [1,2] such as columns, beams, slabs, walls, tunnels, chimneys, and silos, and can be used to improve flexural and shear capacities, and also provide confinement and ductility to compression members.

In order to take full advantage of the potential ductility of the RC member, it is desirable to ensure that flexure rather than shear govern ultimate strength. Shear failure is catastrophic and occurs with no advance warning of distress. Many of the existing RC beams have been found to be deficient in shear strength and in need of strengthening. Deficiencies occur due to several reasons such as insufficient shear reinforcement or reduction in steel area due to corrosion, increased service load construction defects. In these situations, it has been shown that externally bonded FRP reinforcement can increase the shear capacity [3–11].

The objectives of this program are to:

1. Investigate the shear behavior and modes of failure of T-section RC beams with shear deficiencies after strengthening with CFRP sheets.
2. Address the factors that affect shear strength, such as wrapping schemes, CFRP amount, 90°/0° ply combination, and CFRP end anchorage.
3. Increase the database on shear strengthening.
4. Improve and validate the design approach previously proposed by the authors [8].

* Corresponding author. Tel.: +1-573-341-4553; fax: +1-573-341-6215.

E-mail address: nanni@umr.edu (A. Nanni).

PII: S0958-9465(99)00051-7

Notation

a shear span
A_f area of CFRP shear reinforcement $= 2t_f w_f$
b_w width of the beam cross-section
d depth from the top of the section to the tension steel reinforcement centroid
d_f effective depth of the CFRP shear reinforcement (usually equal to d for rectangular sections and $d - t_s$ for T-sections)
E_f elastic modulus of FRP (GPa)
f'_c nominal concrete compressive strength (MPa)
f_{fe} effective tensile stress in the FRP sheet in the direction of the principal fibers (stress level in the FRP at failure)
f_{fu} ultimate tensile strength of the FRP sheet in the direction of the principal fibers
L_e effective bond length (mm)
R reduction coefficient (ratio of effective average stress or strain in the FRP sheet to its ultimate strength or elongation)
s_f spacing of FRP strips
t_f thickness of the FRP sheet on one side of the beam (mm)
V_c nominal shear strength provided by concrete
V_f nominal shear strength provided by FRP shear reinforcement (ACI format)
V_n nominal shear strength (ACI format)
V_s nominal shear strength provided by steel shear reinforcement (ACI format)
V_{fd} design shear contribution of CFRP to the shear capacity (Eurocode format)
V_{Rd1} design shear capacity of concrete (Eurocode format)
V_{Rd2} maximum design shear force that can be carried without web failure (Eurocode format)
V_{wd} design contribution of steel shear reinforcement
w_f width of FRP strip
w_{fe} effective width of FRP sheet (mm)
β angle between the principal fiber orientation and the longitudinal axis of the beam
ε_{fe} effective strain of FRP
ε_{fu} ultimate tensile elongation of the fiber material in the FRP composite
ϕ strength reduction factor (ACI format)
γ_f partial safety factor for CFRP materials (Eurocode format)
ρ_f FRP shear reinforcement ratio $= (2t_f/b_w)(w_f/S_f)$

For these objectives, six full-scale, T-section RC beams with shear deficiencies were strengthened in different configurations and tested.

2. Experimental program

In this experimental program, the selected parameters are:

(a) CFRP amount and distribution (continuous sheets versus series of strips); (b) bonded surface (two sides versus U-wrap);

(c) fiber direction combination (90°–0° fiber direction combination versus 90° direction);

(d) end anchorage (U-wrap without end anchor versus with end anchor).

2.1. Test specimens and materials

The experimental program consisted of six full-scale RC beams with a T-shaped cross-section. The specimens were reinforced with longitudinal steel bars with no steel shear reinforcement in the test region to favor shear failure. Specimen details and dimensions are shown in Fig. 1. The materials used for manufacturing the test specimens and their mechanical properties are listed in Table 1.

2.2. Strengthening schemes and test setup

Specimen BT1 was the reference beam. Specimen BT2 was strengthened using continuous surface bonded U-wraps throughout the beam span. The wraps were made of single-ply CFRP sheets with the fiber direction oriented perpendicular to the longitudinal axis of the beam

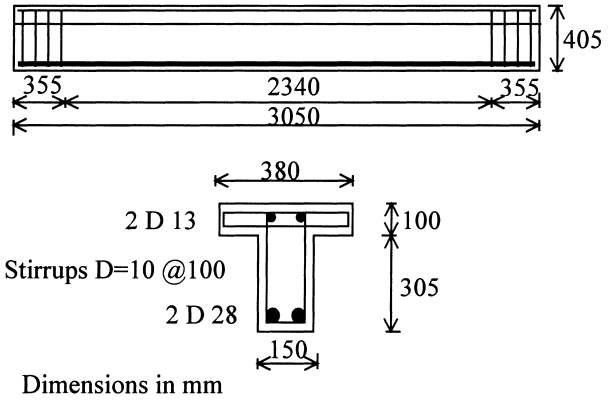

Fig. 1. Beam specimens detailing and dimensions.

Table 1
Beam material properties

Material	Dimensions (mm)	Yield point (MPa)	Compressive strength (MPa)	Tensile strength (MPa)	Modulus of elasticity (GPa)
Concrete	–	–	35	–	–
Steel reinforcing	$D = 28$	470	–	730	200
	$D = 13$	350	–	530	200
	$D = 10$	350	–	530	200
CFRP sheets[a]	$t_f = 0.165$	–	–	3790	228

[a] Fiber only.

(90°). No end anchors were used for specimen BT2. The CFRP wraps were applied following the manufacturer's recommendations [12]. Prior to strengthening, the concrete surface was prepared using water blasting and allowed to dry. It was then coated with a layer of epoxy-based primer, which penetrates the concrete pores and provides better bond properties. After the primer became tack-free, a layer of putty, a thick paste epoxy, was applied to level the surface and patch small holes. A first coat of saturant resin was then applied followed by the fiber sheets. A ribbed roller was used on the sheets to ensure impregnation of the fibers by the saturant. The sheet was then coated with a second layer of saturant resin and the excessive resin was removed.

Specimen BT3 was strengthened with two perpendicular fiber direction plies of CFRP sheets (90°/0°). The first ply was the same as beam BT2. The second ply was bonded to the two beam sides with fiber direction parallel to the beam axis (i.e., 0° direction). The purpose of adding a horizontal ply in 0° direction was to investigate if it had any effect on increasing the beam shear capacity by increasing the shear friction strength along the potential diagonal crack between the load and reaction. The horizontal ply may strengthen the contribution of concrete but will not affect the shear strength of the truss mechanism. In addition, the horizontal ply may act to arrest propagation of vertical cracks starting at the bottom of the section.

Specimen BT4 was strengthened with one-ply CFRP strips in the form of a U-wrap with 90° fiber orientation. The strip width was 50 mm with center-to-center spacing of 125 mm.

Specimen BT5 was strengthened with CFRP strips attached only on the two beams sides with 90° fiber orientation. The strip width and spacing were similar to specimen BT4.

Specimen BT6 was strengthened in a manner similar to that of specimen BT2. The ends of the U-wraps in specimen BT6 were anchored to the flanges on both sides of the beam using the proposed U-anchor system [13]. A cross-section showing details of the U-anchor system is given in Fig. 2. The anchoring was attained by grooving the concrete flanges at the corner. The groove dimensions were about 15×15 mm and extended throughout the strengthened part. The strengthening work was started with concrete surface preparation and priming that includes the walls of the groove. The CFRP sheets were bonded to the concrete surface and to the walls of the groove. After the resin impregnating the sheet (saturant) had set, the groove was filled half way with a high viscosity binder (e.g., epoxy paste) compatible with the FRP system. The high viscosity paste ensures easier field execution, especially in the case of over-head application. A 10 mm diameter Glass FRP rod was then placed into the groove and was lightly pressed in place. This action forces the paste to flow around the sheet and to cover simultaneously part of the rod and the sides of the sheet. The rod was held in place using wedges at the appropriate spacing. The groove was then filled with the same paste and the surface was leveled.

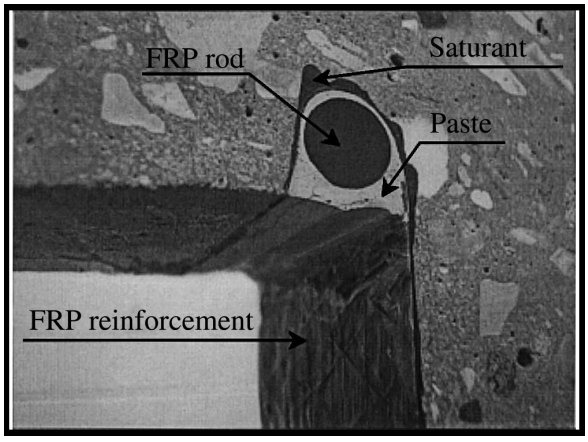

Fig. 2. Details of the U-anchor obtained by slicing a beam.

Strengthening schemes and test setup of the tested beams are shown in Fig. 3. All specimens were tested as simple beams using four-point loading with shear span-to-effective depth ratio (a/d) equal to 3. A loading machine of 1800 kN capacity was used in order to apply a

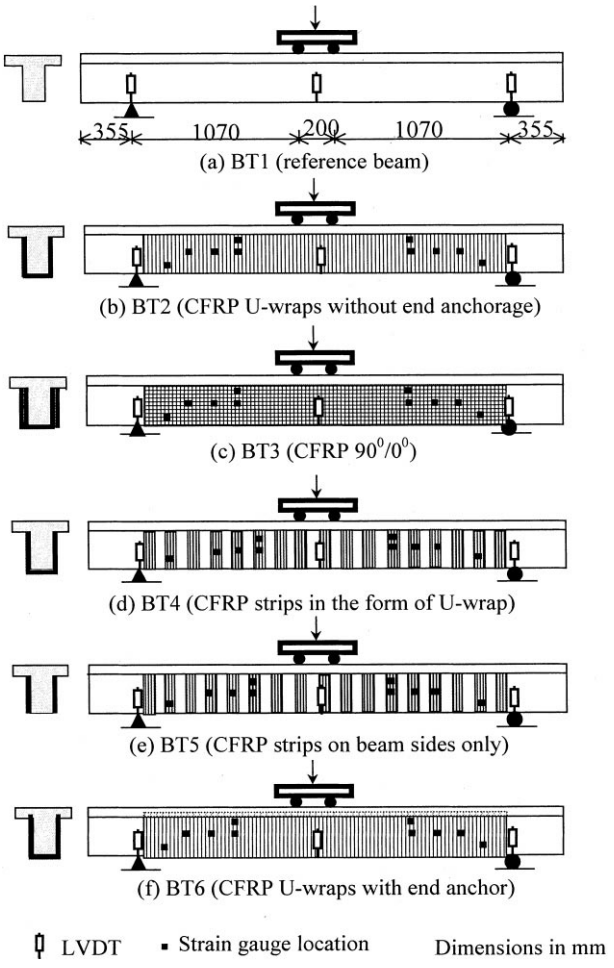

Fig. 3. Test setup and strengthening schemes.

concentrated load on a steel distribution beam used to generate the two concentrated loads. The load was applied in progressively increasing cycles. A cycle before cracking of concrete was done in order to verify whether both the mechanical and electronic equipment were working properly. Two or three cycles before ultimate were done. By applying the load in cycles, the stability of the system can be checked. The applied load versus deflection curves shown in this study are the envelopes of these load cycles. Four linear variable differential transformers (LVDTs) were used for each test to monitor vertical displacements at various locations as shown in Fig. 3. Two LVDTs were located at mid span, one on each side of the beam. The other two were located at the beam supports to record support settlement. Strain gauges were attached to the FRP on the sides of the strengthened beams and oriented in the fiber direction. Ten strain gauges were used for each beam to monitor FRP strain. Strain gauges were mounted at the expected location of shear cracks (as observed in reference beam BT1 during testing). Strain gauge positions are shown in Fig. 3.

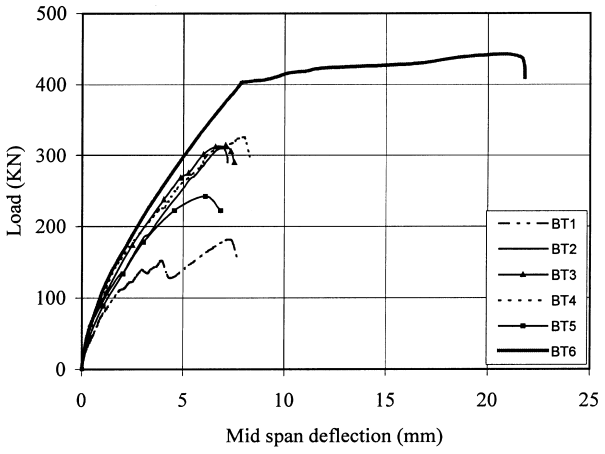

Fig. 4. Experimental results in terms of load-mid span deflection.

3. Test results and discussions

Fig. 4 shows the experimental results in terms of total applied load versus mid span deflection for the tested beams, while the photos in Fig. 5 show the modes of failure of those beams.

When beam BT1 was loaded, it exhibited diagonal shear cracks at a load of 110 kN. The shear cracks started at the center of both shear spans simultaneously. The first shear crack was the critical crack in the beam. As the load increased, this crack started to widen and propagated leading to the eventual failure at a load of 180 kN.

In beam BT2, failure was initiated by debonding of CFRP sheets (with a layer of concrete adhered to them) over the main shear crack in the same location observed in beam BT1. It was followed by shear compression failure at a load of 310 kN. Strengthening of beam BT2 with CFRP U-wraps resulted in a 72% increase in the shear capacity. The maximum localized FRP strain was 0.0045 mm/mm, which corresponds to 28% of the reported ultimate strain of the CFRP. If debonding could be prevented, a better utilization of the strengthening material and consequently a higher increase in shear capacity of the beam would be attained.

In beam BT3 with CFRP (90°/0°), the failure mode was in a similar manner to that of beam BT2. The failure occurred at a total applied load of 315 kN with no significant increase in shear capacity compared to beam BT2. Adding ply in 0° direction over a ply in 90° direction had no effect in increasing the shear capacity of the beam when the failure mode control by FRP debonding. However, the horizontal ply may be effective when the shear span-to-depth ratio is smaller, or when failure mode control by web crashing. Research into quantifying that effect is currently being conducted at the University of Missouri at Rolla (UMR).

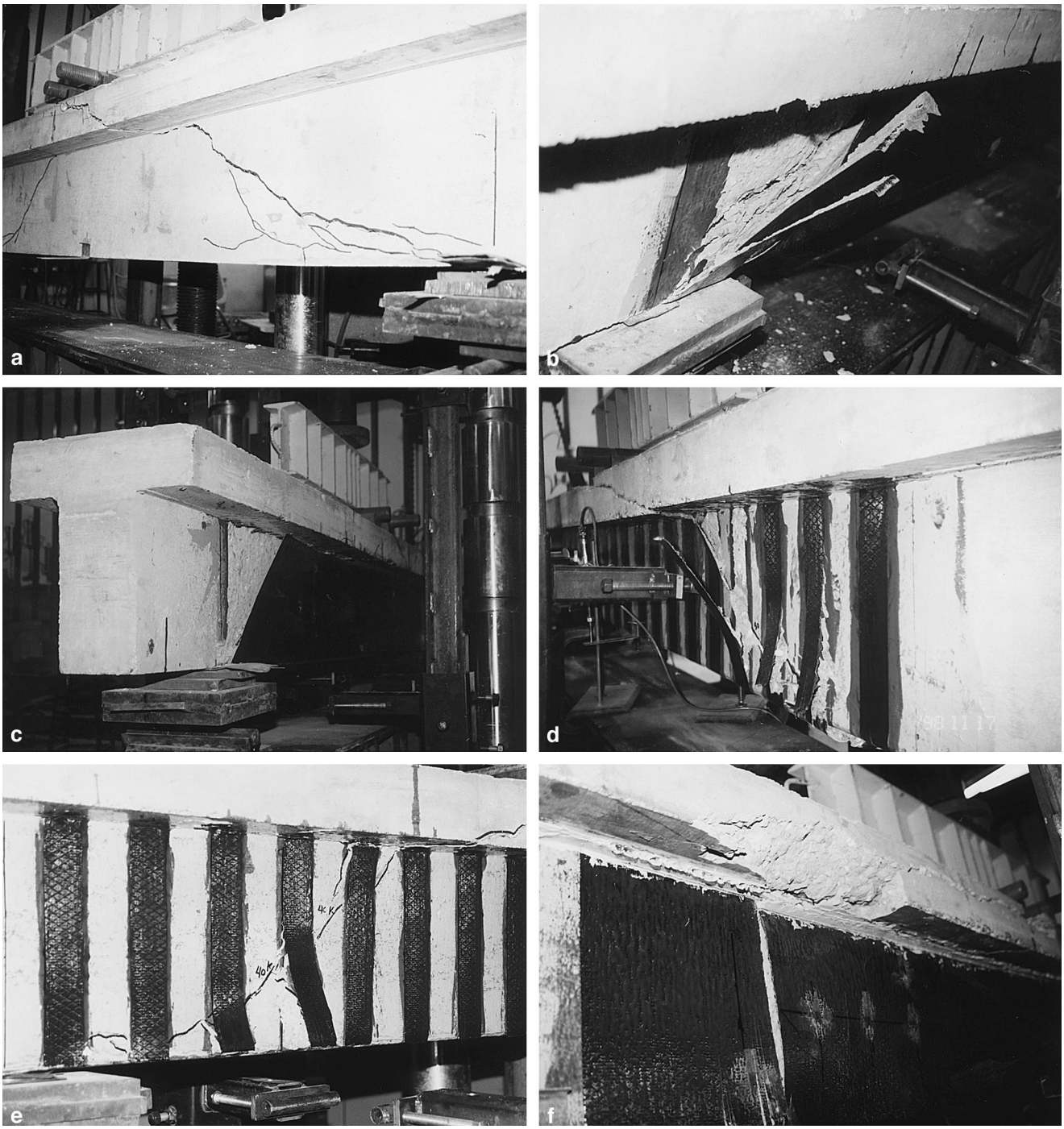

Fig. 5. Failure modes of tested beams.

In beam BT4 with CFRP strips in the form of U-wraps, the diagonal shear crack is observed at a total load of 140 kN. The crack propagated as the load increased in a similar manner to that of beam BT1. The failure occurred due to debonding of CFRP over the main diagonal shear crack, with a concrete layer attached to them, in the area between the center of shear crack and its upper end. This led to an instantaneous increase in the load carried by the other strips located between the shear crack center and its lower end resulting in fracture of two of them followed directly by shear compression failure. The maximum-recorded local vertical strain in CFRP at ultimate was about 0.01 mm/mm which is close to twice the value recorded in the case of continuous sheets, beam BT2. Applied load versus vertical CFRP strain for beam BT4 is shown in Fig. 6.

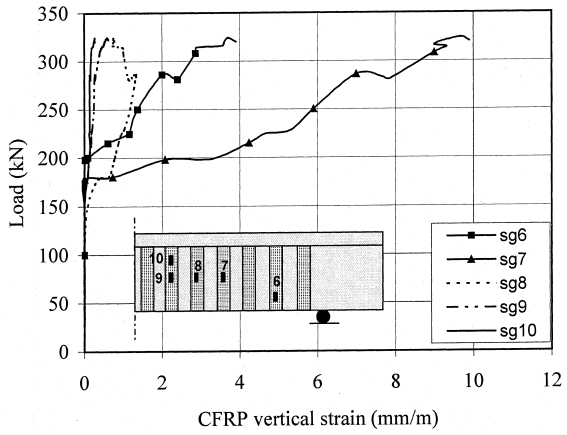

Fig. 6. Load versus vertical CFRP strain for beam BT4.

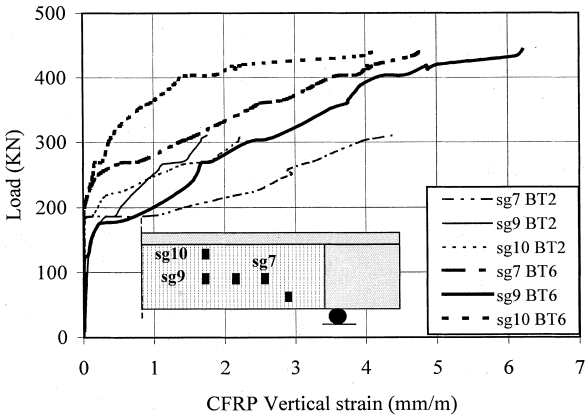

Fig. 7. Load versus vertical CFRP strain for beams BT2 and BT6.

The strain gauges sg6, sg7, sg8, sg9, and sg10 were located at distances of 200, 450, 575, 700, and 700 mm from support, respectively. Sudden failure of beam BT4 occurred at a point load of 324 kN. The load carrying capacity of beam BT4 with CFRP strips is relatively close to that of beam BT2 with continuous sheets. This means that there are optimum FRP quantities, beyond which the strengthening effect cannot be increased. In case of U-wrap continuous sheets, debonding of CFRP sheets from concrete initially starts at the top of diagonal shear crack where the development length is not sufficient. This results in instantaneous increases in load carried by the vicinity. This led to rapid propagation of the debonding of CFRP sheets over the shear crack, combined with beam failure and whatever the quantity of FRP at the vicinity if it was more than or equal to a certain amount. The findings herein closely match those of other researchers. Based on a review of experimental results available in the literature, Triantafillou [9] shows that the contribution of FRP to the shear capacity increases almost linearly with FRP axial rigidity expressed by $\rho_f E_f$ up to approximately 0.4 GPa, beyond which the effectiveness of FRP ceases to be positive.

In beam BT5 with CFRP strips attached to beam sides only, the large diagonal shear crack was formed at a total load of about 140 kN and propagated as the load increased in a similar manner to beams BT1 and BT4. Brittle failure occurred at a total applied load of 243 kN by debonding of CFRP strips followed directly by shear compression failure. The location of debonding area herein is different from beam BT4. In that case, it was below the main shear crack between its center and its lower end. Strengthening of beam BT5 with CFRP strips on the two beam sides resulted in a 35% increase in the shear capacity. Unfortunately, part of the computer file which includes the strain gauge results was lost.

As a result of the use of U-anchors, a significant increase in the shear capacity was achieved in beam BT6. Also, the failure mode at ultimate changed from CFRP debonding (as observed in beam BT2) to flexural failure mode. The measured local maximum vertical strain of the CFRP wrap was 0.0063 mm/mm or 40% of ultimate. This value is not an absolute because it greatly depends on the location of the strain gauge with respect to a crack. Load versus CFRP strain relationships for the two strengthened beams BT2 and BT6 are shown in Fig. 7. The strains at gauges 7, 9, and 10 are plotted. For both beams, shear cracking starts at the same load level; however, a much higher ultimate load (and strain) is attained for BT6. No debonding was observed in the CFRP wrap of beam BT6 at ultimate capacity. After the beam failed in flexure, the CFRP wrap ruptured at the end of the shear crack near the support, as shown in Fig. 5(f). The load carrying capacity of beam BT6 was 442 kN with 145% and 42% increments over the reference beam BT1 and the equally strengthened beam BT2, respectively. Fig. 4 indicates that beam BT6 gained more stiffness and ductility than beam BT2. The additional ductility was obtained from the flexural failure mode. The mid-span deflection of beam BT6 at failure was about 3 times the deflection of beam BT2 at failure.

4. Design approach

The design approach for computing the contribution of externally bonded CFRP reinforcement to the shear capacity of RC beams, in ACI Code [14] format, was proposed in the previous paper [8].

The model described the two possible failure mechanisms of CFRP reinforcement separately (either CFRP fracture or debonding). Furthermore, two limits on the contribution of CFRP shear reinforcement were proposed, the first limit was set to control the shear crack

width and loss of aggregate interlock and the second to preclude web crushing. Also, the concrete strength and CFRP wrapping schemes were considered as design variables.

To quantify the average bond strength and the effective bond length at CFRP debonding, the equations presented by Maeda et al. [15] were used [8]. However, in a recent study, based on experimental and analytical results, Miller [16] modified the model by Maeda et al. and proposed new equations to predict the effective bond length and the ultimate load at CFRP debonding. Although both models seemed to give nearly the same results in terms of ultimate load, a slight modification to improve the shear design algorithms has been proposed [17], including Miller model instead of Meada et al. In addition, the model was extended to provide the shear design algorithms in Eurocode format as well as ACI format. Comparing with all available test results in the literature to date, the design shear model showed acceptable and conservative estimates [17]. The design equations for shear strengthening of RC members with externally bonded CFRP are presented below.

4.1. Shear capacity of a CFRP strengthened section – ACI format

The nominal shear strength of an RC section (V_n) is expressed in Eq. (1).

$$V_n = V_c + V_s + V_f, \tag{1}$$

where V_c is the shear strength of the concrete, V_s the shear strength of the steel reinforcement, and V_f is the shear contribution of the CFRP.

The design shear strength, ϕV_n, is obtained by multiplying the nominal shear strength by a strength reduction factor for shear, ϕ. The ϕ factor for steel and concrete contribution from ACI is 0.85, and the ϕ factor for CFRP contribution is suggested to be 0.70. Eq. (2) presents the design shear strength.

$$\phi V_n = 0.85(V_c + V_s) + 0.7V_f. \tag{2}$$

4.1.1. Contribution of CFRP reinforcement to the shear capacity

The expression to compute CFRP contribution is given in Eq. (3). This equation is similar to that for steel shear reinforcement and is consistent with ACI format.

$$V_f = \frac{A_f f_{fe}(\sin\beta + \cos\beta)d_f}{s_f} \leqslant \left(\frac{2\sqrt{f'_c}b_w d}{3} - V_s\right). \tag{3}$$

In Eq. (3), the area of CFRP shear reinforcement, A_f, is the total thickness of the sheet usually $2t_f$ (for sheets on both sides of the beam) times the width of the CFRP strip w_f. Fig. 8 shows the dimensions used to define the area of CFRP in addition to the spacing s_f and the effective depth of CFRP, d_f. Note that for continuous vertical shear reinforcement, the spacing of the strip, s_f, and the width of the strip, w_f, are equal.

In Eq. (3), a reasonable limit on the maximum amount of additional shear strength that may be achieved is suggested in terms of the shear strength of concrete and steel shear reinforcement. The limit was set to provide adequate safety against web crushing caused by the diagonal compression stress. In addition to the limit, the spacing of CFRP strips should not be so wide to allow the full formation of a diagonal crack without intercepting a strip. For this reason, the strips should not be spaced by more than the maximum given in Eq. (4)

$$S_f \leqslant w_f + d/4. \tag{4}$$

In Eq. (3), the effective CFRP stress, f_{fe}, smaller than its nominal strength, is computed by applying a reduction coefficient, R, to the nominal CFRP strength, f_{fu}, as expressed in Eq. (5).

$$f_{fe} = Rf_{fu}. \tag{5}$$

The reduction coefficient is dependent on the governing mode of failure. Either fracture of CFRP reinforcement at average stress level below nominal strength due to stress concentrations (failure mode 1) or debonding of the CFRP reinforcement from the concrete surface (failure mode 2) governs failure. In either case, an upper limit of reduction coefficient is established in order to

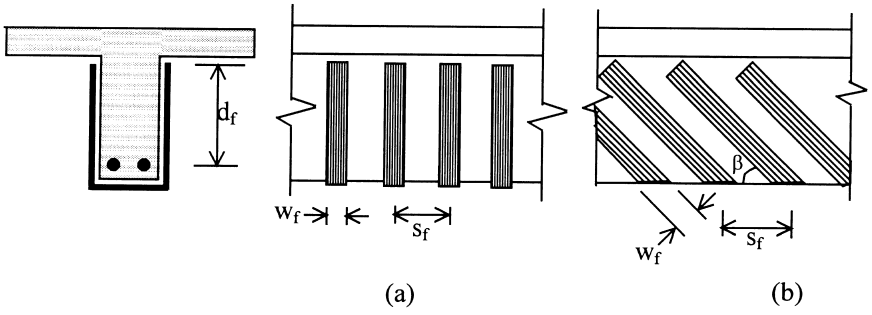

Fig. 8. Dimensions used to define the area of FRP. (a) Vertical oriented FRP strips. (b) Inclined strips.

control shear crack width and loss of aggregate interlock.

4.1.2. Reduction coefficient for failure mode 1

The proposed reduction coefficient for failure mode 1 was based on the experimental results and the works cited presented by Triantafillou [9]. However, modifications were suggested [8] due to additional experimental data that have become available. The proposed reduction coefficient is a function of CFRP stiffness and expressed in Eq. (6) for $\rho_f E_f \leqslant 0.7$ GPa.

$$R = 0.5622(\rho_f E_f)^2 - 1.2188(\rho_f E_f) + 0.778. \quad (6)$$

Although Eq. (6) has been derived from calibration of 48 test results including the two modes of failure, it showed a good agreement and fit all of the available test results in the literature till date (76 test results including 22 in which the failure was controlled by CFRP fracture) [17].

4.1.3. Reduction coefficient for failure mode 2

The shear capacity governed by CFRP debonding from the concrete surface was presented [17] as a function of CFRP stiffness, concrete strength, effective depth of CFRP reinforcement, and bonded surface configurations. In determining the reduction coefficient for bond, the effective bond length, L_e, has to be determined first. Based on analytical and experimental data from bond tests, Miller [16] showed that the effective bond length increases as CFRP stiffness, $E_f t_f$, increases. However, he suggested a conservative value for L_e equal to 75 mm. The value may be modified when more bond tests data become available.

When a shear crack develops, only that portion of the width of CFRP extending past the crack by the effective bonded length has been assumed to be capable of carrying shear [8]. The effective width, W_{fe}, is based on the shear crack angle, assumed to be 45^0, and the wrapping scheme. The value of W_{fe} is expressed in Eqs. (7a) and (7b)

$$W_{fe} = d_f - L_e \quad \text{if the sheet is in the form of a U-wrap,} \quad (7a)$$

$$W_{fe} = d_f - 2L_e \quad \text{if the sheet is bonded only to the sides of the beam.} \quad (7b)$$

The final expression for the reduction coefficient, R, for the mode of failure controlled by CFRP debonding is expressed in Eq. (8)

$$R = \frac{(f'_c)^{2/3} w_{fe}}{\varepsilon_{fu} d_f} [738.93 - 4.06(E_f t_f)] \times 10^{-6}. \quad (8)$$

Eq. (8) is applicable for CFRP stiffness, $E_f t_f$, ranged from 20 to 90 MM-GPa. Research into quantifying the bond characteristics for stiffness above 90 MM-GPa is being conducted at UMR.

4.1.4. Upper limit of the reduction coefficient

In order to control the shear crack width and loss of aggregate interlock, an upper limit of reduction coefficient ($R = 0.5$) was suggested [8]. This limit is such that the effective strain, ε_{fe}, is of the order of 0.005 mm/mm (including the ϕ factor) for CFRP sheets having an ultimate strain, ε_{fu}, in the order of 0.015 mm/mm. Due to the variety of the ultimate strain of CFRP sheets available in the market, a constant upper limit of effective strain was suggested [17] to be about 0.004 mm/mm (including the ϕ factor). Using this value, the upper limit of reduction coefficient, R, is taken to be equal to $0.006/\varepsilon_{fu}$.

4.1.5. Controlled reduction coefficient

The final controlled reduction coefficient for the CFRP system is taken as the lowest value determined from the two possible modes of failure and the upper limit.

For the cases of U-jacket with end anchorage and totally wrap configurations, the failure mode of CFRP debonding is not to be considered. The reduction coefficient is only controlled by FRP fracture and the upper limit.

4.1.6. Concrete surface preparation

It is important to mention that the mechanical concrete surface preparation method (sand blasting, water blasting, or grinder) has a significant effect on the bond behavior of FRP. A primer study at UMR showed that making a small groove using hammer and chisel in parts of the beam surface in which the bond is critical in addition to using the sand blasting, may increase significantly the FRP contribution. However, research into linking the bond behavior of FRP with the degree of concrete surface roughness will be conducted at UMR. Consequently, further improvement to the shear design model to consider that effect will arise.

4.2. Shear capacity of a CFRP strengthened section – Eurocode format

The proposed design (Eq. (3)) for computing the contribution of externally bonded CFRP reinforcement may be rewritten in Eurocode (EC2 1992) [18] format as Eq. (9)

$$V_{fd} = \frac{A_f(f_{fe}/\gamma_f)(0.9d_f)(1 + \cot\beta)\ \sin\beta}{s_f} \leqslant [V_{Rd2} - (V_{Rd1} + V_{wd})], \quad (9)$$

where V_{fd} is the design shear contribution of CFRP to the shear capacity in Eurocode format, γ_f the partial

Table 2
Comparison between test results and calculated values

Specimen	Strengthening schemes	Experimental results			Design approach (ACI format)				
		$V_{n,exp}$ (kN)	$V_{f,exp}$ (kN)	Failure mode at ultimate	V_f (kN)	$V_n = V_c + V_f$ (kN)	$\phi V_f(\phi = 0.7)$ (kN)	$\phi V_n = 0.85V_c + 0.7V_f$ (kN)	Predicted failure mode
BT1	–	90	–	Shear compression	–	57	–	48.45	Shear compression
BT2	Continuous sheets in the form of U-wraps	155	65	CFRP debonding	84.8	141.8	59.3	107.75	CFRP debonding
BT3	Two plies (90°/0°)	157.5	67.5	CFRP debonding	84.8	141.8	59.3	107.75	CFRP debonding
BT4	Strips in the form of U-wraps	162	72	CFRP debonding	33.7	90.7	23.6	72	CFRP debonding
BT5	Strips on the two beam sides only	121.5	31.5	CFRP debonding	19.7	76.7	13.8	62.2	CFRP debonding
BT6	Continuous U-wraps with end anchor	221	>131	Flexure	103.5	160.5	72	120.45	Flexure

safety factor for CFRP materials (suggested equal to 1.3), V_{Rd2} the maximum design shear force that can be carried without web failure, V_{Rd1} is the design shear capacity of concrete, and V_{wd} is the design contribution of steel shear reinforcement.

4.3. Comparison between test results and calculated values

The comparison between the test results and calculated shear strength using the proposed design approach (ACI format) are listed in Table 2. The measured nominal CFRP shear contribution to the shear capacity was obtained by subtracting the ultimate shear strength of the reference beam from the non-strengthened one. Per ACI 318-95 [14, Eq. (11.5)], the nominal shear strength provided by concrete, V_c is equal to 57 kN in Eq. (11.5), the values of V_u and M_u were taken at point of applied load). Moreover, the design shear strength provided by concrete, ϕV_c, is equal to 48.45 kN (considering $\phi = 0.85$). The comparison indicated that the design approach gives acceptable and conservative results.

5. Conclusions

In this study, the shear performance of T-section RC beams with shear deficiencies, strengthened with different configurations of CFRP sheets were investigated. The test results indicated that the externally bonded CFRP reinforcement can be used to enhance the shear capacity of the beams. For the beams tested in the experimental program, increase in shear strength of 35–145% was achieved.

Within the indicated scope of investigation, the particular conclusions that emerged from this study may be summarized as follows:

- The performance of externally bonded CFRP can be improved significantly if adequate anchoring is provided.
- The proposed U-anchor system is recommended where bond and/or development length of FRP are critical according to the design procedure.
- Applying CFRP on the beam sides only gives less shear contribution compared to U-wrap.
- Although the CFRP amount in beam BT4 was 40% of that used in beam BT2, the same strengthening effect was attained. The result mean that there is optimum FRP quantities, beyond that the strengthening effectiveness is questionable.
- CFRP strips, although may be as effective as continuous CFRP sheets in the laboratory, are not recommended by the authors for field application. Continuous sheets may be safer than strips because the damage to an individual strip would have more of an impact on the overall shear capacity.

- No contribution to the shear strength was observed for 0° ply in this test specimen.
- Comparing with the test results, the shear design algorithm provides acceptable and conservative estimates.

6. Suggestions for future research

- To optimize the design algorithm, more beams still need to be tested with different CFRP amount.
- Effect of existing transverse steel reinforcement, shear span-to-effective depth ratio, and adding a ply of FRP in 0° direction over ply in 90° on the shear contribution of CFRP need to be considered in the proposed design algorithms.
- Strengthening effectiveness of U-wrap with/without end anchor in negative moment region has to be investigated for T-section RC beams.
- In order to validate the use of U-wrap with the proposed end anchor in seismic retrofitting situations, the strengthening effectiveness of this system needs to be tested under a cyclic load.
- The shear design algorithm needs to be extended to include strengthening with Aramid FRP and Glass FRP sheets in addition to CFRP.

Acknowledgements

This work was conducted with partial support from the National Science Foundation Industry/University Cooperative Research Center on Repair of Buildings and Bridges with Composites based at the University of Missouri, Rolla. The Egyptian Cultural and Educational Bureau, Washington, DC provided support to the first author.

References

[1] ACI Committee 440, State-of-the-art Report on Fiber Reinforced Plastic (FRP) Reinforcement for Concrete Structures, American Concrete Institute, Detroit, Michigan, 1996. 68 pp.

[2] Fukuyama H, Nakai H, Tanigaki M, Uomoto T. JCI State-of - the-Art on retrofiting by CFRM part1. Materials, construction and application. In: Non-metallic (FRP) reinforcement for concrete structures, Proceedings of the Third Symposium, Japan, vol. 1, October 1997. p. 605–12.

[3] Uji K. Improving shear capacity of existing reinforced concrete members by applying carbon fiber sheets. Trans Jpn Concrete Inst 1992;14:253–66.

[4] Swamy RN, Mukhopadhyaya P, Lynsdale CJ. Strengthening for shear of RC beams by external plate bonding. Struct Eng 1999;77(12):19–30.

[5] Chajes MJ, Januska TF, Mertz DR, Thomson TA, Finch WW. Shear strengthening of reinforced concrete beams using externally applied composite fabrics. ACI Struct J 1995;92(3):295–303.

[6] Arduini M, Nanni A, DiTommaso A, Focacci F. Shear response of continuous RC beams strengthened with carbon FRP sheets. In: Non-metallic (FRP) reinforcement for concrete structures, Proceedings of the Third Symposium, Japan, vol. 1, October 1997. p. 459–66.

[7] Taerwe L, Khalil H, Matthys S. Behavior of RC beams strengthened in shear by external CFRP sheets. In: Non-metallic (FRP) reinforcement for concrete structures, Proceedings of the Third Symposium, Japan, vol. 1, October 1997. p. 483–90.

[8] Khalifa A, Gold W, Nanni A, Abdel-Aziz MI. Contribution of externally bonded FRP to the shear capacity of RC flexural members. J Comp Construct – ASCE 1998;2(4):195–202.

[9] Triantafillou TC. Shear strengthening of reinforced concrete beams using epoxy-bonded FRP composites. ACI Struct J 1998; 95(2):107–15.

[10] Sato Y, Ueda T, Kakuta Y, Tanaka T. Ultimate shear capacity of reinforced concrete beams with carbon fiber sheets. In: Non-metallic (FRP) reinforcement for concrete structures, Proceedings of the Third Symposium, Japan, vol. 1, October 1997. p. 499–506.

[11] Sato Y, Katsumata H, Kobatake Y. Shear strengthening of existing reinforced concrete beams by CFRP sheet. In: Non-metallic (FRP) reinforcement for concrete structures, Proceedings of the Third Symposium, Japan, vol. 1, October 1997, p. 507–14.

[12] MBrace composite strengthening system: engineering design guidelines, second ed. Cleveland (OH): Master Builders Technologies, 1998. 140 pp.

[13] Khalifa A, Alkhrdaji T, Nanni A, Lansburg A. Anchorage of surface mounted FRP reinforcement. Concrete Int – ACI 1999;21(10):49–54.

[14] ACI Committee 318, Building code requirements for structural concrete (ACI 318-95) and commentary (ACI 318R-95), American Concrete Institute, Detroit, 1995. 369 pp.

[15] Maeda T, Asano Y, Sato Y, Ueda T, Kakuta Y. A study on bond mechanism of carbon fiber sheet. In: Non-metallic (FRP) reinforcement for concrete structures, Proceedings of the Third Symposium, Japan, vol. 1, October 1997. p. 279–86.

[16] Miller, BD. Bond between carbon fiber reinforced polymer sheets and concrete. MSc Thesis, Department of Civil Engineering, The University of Missouri, Rolla, MO, 1999.

[17] Khalifa A. Shear behavior of reinforced concrete beams strengthened with externally bonded composites. Ph.D. Thesis, Structural Engineering Department, Alexandria University, Egypt, 1999.

[18] Eurocode No. 2, Design of concrete structures, European Committee for Standardization, Lausanne, 1992.